Study of Zn(O,S) Films grown by Aerosol Assisted Chemical Vapour Deposition and their Application as Buffer Layers in Cu(In,Ga)(S,Se)$_2$ Solar Cells

Merike Kriisa[1,2], Rodrigo Sáez-Araoz[1], Christian-Herbert Fischer[1,3], Tristan Köhler[1], Erki Kärber[2], Yanpeng Fu[1], Frank Hergert[4] , Martha Christina Lux-Steiner[1,5], Malle Krunks[2]

[1] Institute for Heterogeneous Material Systems, Helmholtz Centre Berlin for Materials and Energy, Hahn-Meitner-Platz 1, 14109 Berlin, Germany

[2] Laboratory of Thin Film Chemical Technologies, Department of Materials Science, Tallinn University of Technology, Ehitajate tee 5, 19086 Tallinn, Estonia

[3] Freie Universität Berlin, Institut für Chemie, Fabeckstr. 34-36, 14195 Berlin, Germany

[4] Bosch Solar CISTech GmbH, Muenstersche Str. 24, 14772 Brandenburg an der Havel, Germany

[5] Fachbereich Physik, Freie Universität Berlin, Arnimallee 14, 14195 Berlin, Germany

Keywords: chalcopyrite thin film solar cells; Zn(O,S); Cd-free buffer layer; aerosol assisted chemical vapour deposition (AACVD)

Corresponding author: Merike Kriisa, Tel: +372 6203369, Fax: +372 6202020, Email: merike.kriisa@ttu.ee

Abstract

To reduce the use of toxic and expensive elements in chalcopyrite thin film solar cells, materials such as cadmium or indium used in buffer layers need to be substituted. Zn(O,S) is considered to be a potential buffer layer material when deposited with a fast and inexpensive method. Zn(O,S) layers have been prepared by aerosol assisted chemical vapour deposition (AACVD) technique. AACVD technique is a simple non-vacuum process where the thin film deposition temperatures do not exceed 250°C. 10 mM spray solution was made by dissolving zinc(II)acetylacetonate monohydrate in ethanol. The films were grown on Mo substrate at 225°C (film growth temperature). The effect of deposition parameters (spray solution concentration, N$_2$ flow rate, H$_2$S flow rate) on Zn(O,S) thin film properties were studied with SEM and XRD. Thereupon optimizing the deposition parameters, homogeneous and compact Zn(O,S) thin films were obtained and the films were employed in the chalcopyrite thin film solar cell structure by growing films on Cu(In,Ga)(S,Se)$_2$ substrates industrially produced by BOSCH Solar CISTech GmbH. The resulting cells were studied using current-voltage and quantum efficiency analysis and compared with solar cell references that include In$_2$S$_3$ and CdS as buffer layer deposited by ion layer gas reaction and chemical bath deposition, respectively. The best output of the solar cell containing Zn(O,S) as buffer layer and without intrinsic ZnO under standard test conditions (AM 1.5G, 100 mW/cm^2, 25°C) is: Voc=573 mV, Jsc=39.2 mA/cm^2, FF=68.4% and efficiency of 15.4% being slightly better than the In$_2$S$_3$ or CdS containing solar cell references.

Keywords: Aerosol assisted chemical vapour deposition; Zn(O,S); buffer layer; solar cell

1. Introduction

Manufacturing solar cells that have high efficiency while consisting of cost-effective and environmentally friendly materials is of great interest. Therefore, the amount of In and Cd in the chalcopyrite-based solar cell structures needs to be reduced. Due to their abundance and harmlessness Zn compounds can be potential candidates to be used as buffer layers in solar cell structures (Ennaoui et al., 2003; Kushiya, 2014; Merdes et al., 2009). For the last decade, Zn(O,S) has been used as an effective, non-toxic, cost-efficient buffer layer in solar cell structures (Buffière et al., 2011; Ennaoui, 2006; Grimm et al., 2010; Hultqvist et al., 2009; Klenk et al., 2013; Platzer-Björkman et al., 2006; Ramanathan et al., 2012; Sáez-Araoz et al., 2008; Witte et al., 2013). Using Zn(O,S) in solar cell as buffer layer gives also the opportunity to omit the intrinsic ZnO window layer in the solar cell structure and therefore making the solar cell structure and production simpler and cheaper.

So far, Zn(O,S) layers have been prepared by methods that are either slow, not in-line suitable or vacuum techniques, such as chemical bath deposition (CBD) (Buffière et al., 2011; Kushiya, 2004; Sáez-Araoz et al., 2008; Witte et al., 2013), atomic layer deposition (ALD) (Platzer-Bjorkman et al., 2003; Platzer-Björkman et al., 2006; Sanders and Kitai, 1992; Zimmermann et al., 2006), sputtering (Grimm et al., 2011, 2010; Klenk et al., 2013; Kobayashi et al., 2013; Nakamura et al., 2013). The best efficiencies for solar cells with sputtered or ALD deposited Zn(O,S) buffer layer are similar, 18.3% and 18.5% respectively (Klenk et al., 2013; Zimmermann et al., 2006). At the moment, the highest reported CBD deposited Zn(O,S) buffered solar cell efficiency is 20.9% (Kushiya, 2014). In this study, a simple, fast and cost-efficient atmospheric pressure aerosol assisted chemical vapour deposition (AACVD) was used. The AACVD is a simple non-vacuum process where the deposition temperatures do not exceed 250°C (Fischer et al., 2011) and the deposition of the solar cell component is a continuous operation; breaking of the vacuum for the P2 scribing (second scribing step in monolithically integrated devices) between intrinsic ZnO (i-ZnO) and n-type (n-ZnO), that is necessary for the regular solar cell structure where P2 is applied after the i-ZnO deposition, is avoided.

Due to a higher band gap, the Zn(O,S) buffers have the advantage of absorbing less blue light from the sun spectrum than the state of the art CdS buffer layers, therefore reducing the losses in that wavelength region. The reported band gap of ALD and CBD deposited Zn(O,S) layers are 3.6 eV (Sanders and Kitai, 1992) and 3.7 eV (Buffière et al., 2011), respectively. The band gap of sputtered Zn(O,S) has a parabolic dependency with the S/(S+O) ratio varying from 2.6 eV to 3.6 eV (Grimm et al., 2011; Kobayashi et al., 2013). Naturally, the S/(S+O) ratio influences the structural and optical properties of Zn(O,S) layers (Grimm et al., 2011; Kobayashi et al., 2013; Platzer-Björkman et al., 2006). An increase in the sulphur content from 0 to 1 in the $Zn(O_{1-x},S_x)$ film follows the Vegard's law (Vegard, 1921) and results in X-ray diffraction peaks characteristic to ZnS.

This is the first publication of AACVD grown Zn(O,S) layers and the aim is to study the effect of reactive gas concentration and carrier gas flow rate on the morphological, structural and optical properties of Zn(O,S) layers deposited by AACVD on Mo substrates. Furthermore, the solar cell characteristics of $Cu(In,Ga)(S,Se)_2$ devices with AACVD grown Zn(O,S) as buffer layer are discussed.

2. Experimental

2.1. Zn(O,S) layer deposition

Zn(O,S) layers were deposited by AACVD onto preheated molybdenum coated soda lime glass substrates (2.5 x 2.5 cm^2). Prior to each deposition, the glass/molybdenum (gl/Mo) substrates

were cleaned by rinsing with technical ethanol. 10 mmol/L zinc(II)acetylacetonate solution ($C_{10}H_{14}O_4Zn \cdot H_2O$, Alfa Aesar, ≥98%, dissolved in ethanol, abs., ≥99.8%) was used as the zinc precursor solution. This solution is nebulised by an ultrasonic atomiser and the aerosol is blown towards the preheated substrate by a laminar flow of the carrier gas N_2 at a constant angle of 45°. The N_2 flow rate was 5 L/min or 7 L/min. To grow Zn(O,S) layers, the deposition time and temperature (T) are kept constant at 30 minutes and at 225°C using a feedback control system for the heater supply, respectively. 5% H_2S in Ar (flow rate varied from 0 mL/min up to 20 mL/min) is introduced as the reactant gas into the aerosol stream towards the heated substrate. Above the heated substrate the solvent droplets vaporise and the desired film is formed on the substrate. The scheme of the aerosol assisted chemical vapour deposition set-up used in this study is presented in Fig. 1.

2.2. Zn(O,S) layer characterisation

The surface morphology of Zn(O,S) layers on glass/Mo substrate was characterised by scanning electron microscopy (SEM). In addition, the film thickness was obtained from the SEM cross-sectional images using a Gemini LEO1530. X-ray diffractions of Zn(O,S) layers on gl/Mo substrate were recorded with grazing incidence using a Bruker D8 diffractometer with a CuKα-source (λ = 1.5406 Å). To study the optical properties, the Zn(O,S) layers were deposited onto quartz substrate and measured using a *Cary 500* Spectrophotometer equipped with an integrating sphere. The Zn(O,S) band gap was determined from absorption and reflection measurements by the Tauc-Plot.

2.3. Solar cell preparation

In order to obtain solar cells, Zn(O,S) layers were deposited by AACVD on glass/Mo/Cu(In,Ga)(S,Se)$_2$ (CIGSSe) substrates obtained from BOSCH Solar CISTech GmbH Germany (2.5 x 2.5 cm^2) and cleaned by rinsing with ethanol. Thereupon, Al-doped ZnO (AZO) was directly sputtered on half of the number of solar cells while the other half had radio frequency (rf) deposited intrinsic ZnO (i-ZnO) in addition to AZO layers on top of the AACVD Zn(O,S) buffer layer. Finally, Ni/Al grid contacts were deposited on the solar cells to improve the collection. Hence, two solar cell structures were formed: glass/Mo/CIGSSe/AACVD-Zn(O,S)/AZO/ and glass/Mo/CIGSSe/AACVD-Zn(O,S)/i-ZnO/AZO/, designated as **structure 1** and **structure 2**, respectively. For references, solar cells with CdS and In$_2$S$_3$ buffer layers were deposited by CBD and ion layer gas reaction (ILGAR), respectively.

2.3. Solar cell performance

The solar cell performance (scribed total area of 0.5 cm^2, 8 cells per sample) was tested with a class A sun simulator under standard test conditions (25°C, 100 mW/cm^2, AM1.5G) and an external quantum efficiency apparatus.

3. Results and discussions

3.1. Properties of Zn(O,S) layers

The morphology of Zn(O,S) layers deposited with different H_2S flow rates while other deposition parameters were constant (M_{Zn}=10 mmol/L, T=225°C, N_2 flow rate of 5 L/min, deposition time 30 minutes) was studied with SEM. The surface morphology of Zn(O,S) layers depends strongly on the flow rate and therefore on the concentration of the purging gas (H_2S): higher reactive gas concentrations lead to powdery films. It can be seen that increasing the flow rate of the reactive gas from 2 mL/min (Fig. 2a) to 3 mL/min (Fig. 2b) has a small effect yet

slightly increases the number and the size of particles on top of a compact Zn(O,S) surface. With further increase of H_2S flow rate to 10 mL/min the number of particles on the surface increases; their size reaches a maximum diameter of ca. 1 µm (Fig. 2c). The film thickness decreases from 55 nm to 45 nm with the increase of H_2S flow rate from 2 mL/min to 3 mL/min, respectively. Therefore, using the following deposition parameters leads to relatively compact Zn(O,S) layer: M_{Zn}=10 mmol/L, T=225°C, N_2 flow rate of 5 L/min, deposition time 30 min and the flow rate of purging gas is 2 mL/min (**recipe 1**).

The formation of the powdery particles on top of the Zn(O,S) layer can be caused by the formation and precipitation of ZnS already either in the droplet or from the gas phase. This is supported by the increasing number of particles on the surface with increasing the H_2S flow rate, as can be seen in Fig. 2 a)-c).

From our previous study (Fischer et al., 2011) we know that increasing the carrier gas flow rate shortens the residence time of the aerosol over the substrate. Therefore, we increased the N_2 flow rate from 5 L/min to 7 L/min and used the H_2S flow rate of 5 mL/min (**recipe 2**) while other deposition parameters were as mentioned in the beginning of this section. These deposition conditions led to a compact and homogeneous Zn(O,S) with very little particles on the film surface (Fig. 2d) and to film thickness of 60 nm. These films are thicker due to the higher amount of aerosol transported to the heated sample.

Crystalline films were obtained independently of the used recipe. The X-ray diffraction patterns of AACVD deposited Zn(O,S) layers on gl/Mo substrate according to **recipe 2** and the ZnO and ZnS powder references (*International Centre for Diffraction Data*, 2008) are shown in Fig. 3. It can be seen that the XRD peaks characteristic to Zn(O,S) are more similar to wurtzite ZnS (PDF card No. 01-075-1534) rather than to hexagonal ZnO (PDF card No. 01-079-0208).

The optical transmittance, reflectance and the absorbance of Zn(O,S) deposited according to **recipe 2** on quartz substrate in the visible range of the spectrum is ca. 70%, ca. 20% and ca. 10%, respectively (Fig. 4a). The direct band gap of Zn(O,S) layer is approximately 3.6 eV (Fig. 4b) being slightly higher than the Eg value presented by (Sanders and Kitai, 1992) for ALD deposited Zn(O,S) films with sulphur to zinc ratio of 0.9.

3.2. Characteristics of solar cells with Zn(O,S)

The Zn(O,S) buffered solar cells (deposited according to **recipe 1**) were tested in two solar cell structures: **structure 1** (glass/Mo/CIGSSe/AACVD-Zn(O,S)/AZO) and **structure 2** (glass/Mo/CIGSSe/AACVD-Zn(O,S)/i-ZnO/AZO). The solar cell parameters (Voc, Jsc, FF and η) are presented in Fig. 5. It is visible that using rf intrinsic ZnO in the solar cell structure results in output parameters that have lower deviation from the mean value (Fig. 5 **structure 2**) compared to solar cells without rf-deposited i-ZnO (Fig. 5 **structure 1**). Still, there is no significant difference in the best cell parameters between **structure 1** and **structure 2** (Fig. 5). Omitting the rf-deposited i-ZnO window layer from the solar cell structure allows us to simplify the solar cell structure. Therefore, the deposition process would become simpler, cheaper and faster leading to decreased solar cell production cost being attractive in a solar module production, where for the P2 scribe line application in between sputtered i-ZnO and n-ZnO the vacuum has to be broken.

The output parameters of references, CdS and In_2S_3 buffered solar cells, are also presented in Fig. 5. Independent of the solar cell structure with Zn(O,S) as buffer layer, the best solar cell output parameters are comparable with In_2S_3 and CdS buffered solar cells although the deviation from the mean value is high. The best solar cell output parameters with Zn(O,S) as

the buffer layer are Voc=573 mV, Jsc=39.2 mA/cm^2, FF=68.4% and η=15.4% (Fig. 5 and Table 1). In 2003, (Platzer-Bjorkman et al., 2003) presented the study of solar cells (area <1 cm^2) with ALD deposited Zn(O,S) buffer layers where the Voc is 684 mV, Jsc=32 mA/cm^2, FF=73% and η=16%. The higher solar cell output parameter values with ALD grown Zn(O,S) buffer layer are possibly due to more homogeneous Zn(O,S) layer.

A decrease in layer deposition time from 30 minutes to 20 minutes to grow Zn(O,S) films according to **structure 1** and **recipe 1**, increases slightly the Voc and FF and therefore also the efficiency of a solar cell (see Fig. 5 and Table 1). For **recipe 2**, all the solar cell output parameter values decrease slightly when the deposition time is decreased to 20 minutes. The main loss in the Zn(O,S) buffered solar cell efficiency between **recipe 1** and **recipe 2** is originated from the fill factor, up to 16% lower fill factor is characteristic to solar cells with Zn(O,S) buffer layer grown according to **recipe 2** compared to **recipe 1**.

Independent of the deposition time, the efficiency of Zn(O,S) buffered solar cell grown according to **recipe 1** is comparable with reference solar cells (14.9% for solar cell with Zn(O,S) grown for 30 minutes, 15.4% for solar cell with Zn(O,S) grown for 20 minutes and 15.2% for In$_2$S$_3$ or 14.6% for CdS buffered solar cells) (Table 1). While the Jsc and FF are comparable to the reference solar cells parameters, the main difference is in the Voc. Independent of the deposition time, the Voc of the Zn(O,S) buffered solar cell is 5-20 mV lower than for the In$_2$S$_3$ or CdS or buffered solar cells (582 mV and 584 mV and, respectively). The output parameters of solar cells with Zn(O,S) buffer layers grown according to **recipe 2**, are lower than the reference values for CdS or In$_2$S$_3$ buffered solar cells, independent of the Zn(O,S) layer deposition time (Table 1). Interestingly, to lower the process cost and time to prepare solar cell, the Zn(O,S) buffer layer could be grown for 20 minutes instead of 30 minutes only according to **recipe 1**.

The external quantum efficiency spectra of Zn(O,S) grown according to **recipe 1** for 30 minutes and CdS buffered solar cells are presented in Fig. 6. The buffer layer thicknesses in these solar cells are comparable at ca. 60 nm. The advantage of the use of Zn(O,S) versus the use of CdS as the buffer layer is evident from the EQE of the respective cells (Fig. 6). The CdS, with a band gap of 2.4 eV, absorbs light in the wavelength region of 380-550 nm resulting in lower quantum efficiency. However, the presence of the Zn(O,S) with a band gap of 3.6 eV, that will transmit light down to its absorbing edge at around 350 nm, does not lead to absorption losses in this wavelength region. It can be speculated that the decline in EQE at around 2.5 eV for Zn(O,S) buffered solar cell can be due to the interference pattern.

4. Conclusions

The Zn(O,S) layers were grown by a simple, cost-efficient and continuous aerosol assisted chemical vapour deposition (AACVD). The surface morphology of AACVD deposited Zn(O,S) is dependent on the flow rate and therefore the concentration of the H$_2$S: flow rates higher than 0.2 mL/min lead to non-homogeneous and non-compact layers. To obtain compact Zn(O,S) layers, the deposition parameters should be 2 mL/min of 5% H$_2$S in Ar and carrier gas flow rate of 5 L/min (**recipe 1**) or 5 mL/min of reactive gas and 7 L/min of carrier gas (**recipe 2**) corresponding to a solution concentration of 10 mmol/L. Values greater than the mentioned parametric numbers lead to powdery and not compact films. XRD patterns show the presence of crystalline matter being similar rather to ZnS than to ZnO. The transmittance of the Zn(O,S) film in the visible spectrum range is ca. 70% and the Eg≈3.6 eV.

The solar cells with Zn(O,S) as the buffer layer were grown on industrial glass/Mo/Cu(In,Ga)(S,Se)$_2$ substrates. The solar cells with Zn(O,S) buffer layer have

comparative solar cell output characteristics with CdS and In$_2$S$_3$ references. The use of Zn(O,S) as a buffer layer in solar cell makes the cell structure and production simpler and cheaper by allowing to omit the intrinsic ZnO from the solar cell structure. Hence, the use of AACVD deposited Zn(O,S) allows to avoid the breaking of vacuum for the P2 scribing (second scribing step in monolithically integrated devices) between i-ZnO and n-ZnO that is necessary for the regular solar module structure (if P2 is applied after the i-ZnO deposition). Decreasing the deposition time from 30 to 20 minutes for the deposition of Zn(O,S) layer according to **recipe 1**, the solar cell output characteristics increase slightly being comparable with the reference CdS and In$_2$S$_3$ buffered solar cell output parameters. Yet at the moment the variation in deposition time has not been optimised for the lab scale depositions but the results are promising. Nevertheless, Zn(O,S) can be used as a buffer layer in solar cells without the loss in efficiency while decreasing the cost and time of solar cell production instead of costly In and toxic Cd used to grow buffer layers in modern solar cells.

Acknowledgements

References

Buffière, M., Harel, S., Arzel, L., Deudon, C., Barreau, N., Kessler, J., 2011. Fast chemical bath deposition of Zn(O,S) buffer layers for Cu(In,Ga)Se$_2$ solar cells. Thin Solid Films 519, 7575–7578. doi:10.1016/j.tsf.2011.01.104

Ennaoui, A., 2006. Highly-efficient Cd-free CuInS2 Thin-film Solar Cells and Mini-modules with Zn(S,O) Buffer Layers Prepared by an Alternative Chemical Bath Process. Prog. PHOTOVOLTAICS 14, 499–511. doi:10.1002/pip

Ennaoui, A., Eisele, W., Lux-Steiner, M., Niesen, T.P., Karg, F., 2003. Highly efficient Cu(Ga,In)(S,Se)$_2$ thin film solar cells with zinc-compound buffer layers, in: Thin Solid Films. pp. 335–339.

Fischer, C.-H., Allsop, N.A., Gledhill, S.E., Köhler, T., Krüger, M., Sáez-Araoz, R., Fu, Y., Schwieger, R., Richter, J., Wohlfart, P., Bartsch, P., Lichtenberg, N., Lux-Steiner, M.C., 2011. The spray-ILGAR® (ion layer gas reaction) method for the deposition of thin semiconductor layers: Process and applications for thin film solar cells. Sol. Energy Mater. Sol. Cells 95, 1518–1526. doi:10.1016/j.solmat.2010.12.019

Grimm, A., Just, J., Kieven, D., Lauermann, I., Palm, J., Neisser, A., Rissom, T., Klenk, R., 2010. Sputtered Zn(O,S) for junction formation in chalcopyrite-based thin film solar cells. Phys. status solidi - Rapid Res. Lett. 4, 109–111. doi:10.1002/pssr.201004083

Grimm, A., Kieven, D., Klenk, R., Lauermann, I., Neisser, A., Niesen, T., Palm, J., 2011. Junction formation in chalcopyrite solar cells by sputtered wide gap compound semiconductors. Thin Solid Films 520, 1330–1333. doi:10.1016/j.tsf.2011.04.150

Hultqvist, A., Platzer-Björkman, C., Pettersson, J., Törndahl, T., Edoff, M., 2009. CuGaSe$_2$ solar cells using atomic layer deposited Zn(O,S) and (Zn,Mg)O buffer layers. Thin Solid Films 517, 2305–2308.

International Centre for Diffraction Data, 2008, PDF-2 Release.

Klenk, R., Steigert, A., Rissom, T., Greiner, D., Kaufmann, C.A., Unold, T., Lux-Steiner, M.C., 2013. Junction formation by Zn(O,S) sputtering yields CIGSe-based cells with efficiencies exceeding 18%. Prog. Photovoltaics Res. Appl. doi:10.1002/pip.2445

Kobayashi, T., Kumazawa, T., Jehl Li Kao, Z., Nakada, T., 2013. Cu(In,Ga)Se$_2$ thin film solar cells with a combined ALD-Zn(O,S) buffer and MOCVD-ZnO:B window layers. Sol. Energy Mater. Sol. Cells 119, 129–133. doi:10.1016/j.solmat.2013.05.052

Kushiya, 2014. Solar Frontier. Press release 2014.

Kushiya, K., 2004. Development of Cu(InGa)Se-based thin-film PV modules with a Zn(O,S,OH) buffer layer. Sol. Energy 77, 717–724. doi:10.1016/j.solener.2004.08.027

Merdes, S., Sáez-Araoz, R., Ennaoui, A., Klaer, J., Lux-Steiner, M.C., Klenk, R., 2009. Recombination mechanisms in highly efficient thin film Zn(S,O)/Cu(In,Ga)S$_2$ based solar cells. Appl. Phys. Lett. 95, 213502. doi:10.1063/1.3266829

Nakamura, M., Kouji, Y., Chiba, Y., Hakuma, H., Kobayashi, T., Nakada, T., 2013. Achievement of 19.7% efficiency with small-sized Cu(InGa)(SeS)$_2$ solar cells prepared by sulfurization after selenization process with Zn-based buffer. Proc. 39th IEEE Photovolt. Spec. Conf. in press.

Platzer-Bjorkman, B., Kessler, J., Stolt, L., 2003. Atomic layer deposition of Zn(O,S) buffer layers for high efficiency Cu(In,Ga)Se$_2$ solar cells. 3rd World Conf. Photovolt. Energy Convers. 461–464.

Platzer-Björkman, C., Törndahl, T., Abou-Ras, D., Malmström, J., Kessler, J., Stolt, L., 2006. Zn(O,S) buffer layers by atomic layer deposition in Cu(In,Ga)Se$_2$ based thin film solar cells: Band alignment and sulfur gradient. J. Appl. Phys. 100, 044506. doi:10.1063/1.2222067

Ramanathan, K., Mann, J., Glynn, S., Christensen, S., Pankow, J., Li, J., Scharf, J., Mansfield, L., Contreras, M., Noufi, R., 2012. A comparative study of Zn(O,S) buffer layers and CIGS solar cells fabricated by CBD, ALD, and sputtering, in: 2012 IEEE Photovoltaic Specialists Conference. IEEE, p. 4. doi:10.1109/PVSC.2012.6317918

Sáez-Araoz, R., Ennaoui, A., Kropp, T., Veryaeva, E., Niesen, T.P., Lux-Steiner, M.C., 2008. Use of different Zn precursors for the deposition of Zn(S,O) buffer layers by chemical bath for chalcopyrite based Cd-free thin-film solar cells. Phys. Status Solidi 205, 2330–2334. doi:10.1002/pssa.200779421

Sanders, B.W., Kitai, A., 1992. Zinc oxysulfide thin films grown by atomic layer deposition. Chem. Mater. 4, 1005–1011. doi:10.1021/cm00023a015

Zimmermann, U., Ruth, M., Edoff, M., 2006. Cadmium-free CIGS min-modules with ALD-grown Zn(O,S)-based buffer layers. 21st Eur. Photovolt. Sol. Energy Conf. 1831–1834.

Vegard, L., 1921. Die Konstitution der Mischkristalle und die Raumfüllung der Atome. Zeitschrift für Phys. 5, 17–26. doi:10.1007/BF01349680

Witte, W., Abou-Ras, D., Hariskos, D., 2013. Chemical bath deposition of Zn(O,S) and CdS buffers: Influence of Cu(In,Ga)Se$_2$ grain orientation. Appl. Phys. Lett. 102, 051607. doi:10.1063/1.4788717

Table 1. The best output parameters for Zn(O,S) buffered solar cells (**structure 1**) with Zn(O,S) grown according to **recipe 1** and **recipe 2** with deposition times of 20 minutes and 30 minutes. The best output parameters of CdS and In_2S_3 buffered cells are given for comparison.

	Deposition time, minutes	Voc, mV	Jsc, mA/cm^2	FF, %	η, %
Recipe 1	20	573	39.2	68.4	15.4
(N_2 of 5 L/min, H_2S of 2 mL/min)	30	572	38.8	66.9	14.9
Recipe 2	20	562	36.9	52.3	10.9
(N_2 of 7 L/min, H_2S of 5 mL/min)	30	577	38.3	56.8	12.5
In_2S_3 reference	N. A.	582	40.4	64.5	15.2
CdS reference	N. A.	584	36.8	67.9	14.6

n.a. – not available

Fig. 1. The scheme of atmospheric pressure aerosol assisted chemical vapour deposition (AACVD) set-up.

Fig. 2. SEM images of Zn(O,S) layers on gl/Mo substrates deposited according to **recipe 1** (N_2 flow rate is 5 L/min) with varied H_2S flow rate of 2 mL/min (a), 3 mL/min (b) and 5 mL/min (c) and Zn(O,S) layer grown according to **recipe 2** (d) with N_2 and H_2S flow rate of 7 L/min and 5 mL/min, respectively.

Fig. 3. X-ray diffractogram of Zn(O,S) deposited according to **recipe 2** (N_2 and H_2S flow rate of 7 L/min and 5 mL/min, respectively), ZnO and wurtzite ZnS powder diffractograms.

Fig. 4. Optical properties (transmittance, reflectance and absorbance) (a) and Tauc plot of Zn(O,S) film on quartz substrate (b) deposited according to **recipe 2**: N_2 and H_2S flow rate of 7 L/min and 5 mL/min, respectively.

Fig. 5. Variance of output parameters of eight 0.5 cm^2 solar cells with Zn(O,S) as buffer layer and reference solar cells with CdS or In_2S_3 as buffer layer. **Structure 1** is glass/Mo/CIGSSe/AACVD-Zn(O,S)/AZO/Ni/Al and **structure 2** is glass/Mo/CIGSSe/AACVD-Zn(O,S)/i-ZnO/AZO/Ni/Al. Zn(O,S) as the buffer layer was deposited according to **recipe 1** for 30 minutes. The output parameter variance of CdS and In_2S_3 buffered cells is given for comparison.

Fig. 6. EQE spectra of thin film solar cells with CIGSSe/Zn(O,S)/AZO and CIGSSe/CdS/i-ZnO/AZO structures. The Zn(O,S) was deposited according to **recipe 1** for 30 minutes. The corresponding Jsc values for Zn(O,S) and CdS buffered solar cells are 38.8 mA/cm^2 and 36.8 mA/cm^2, respectively.
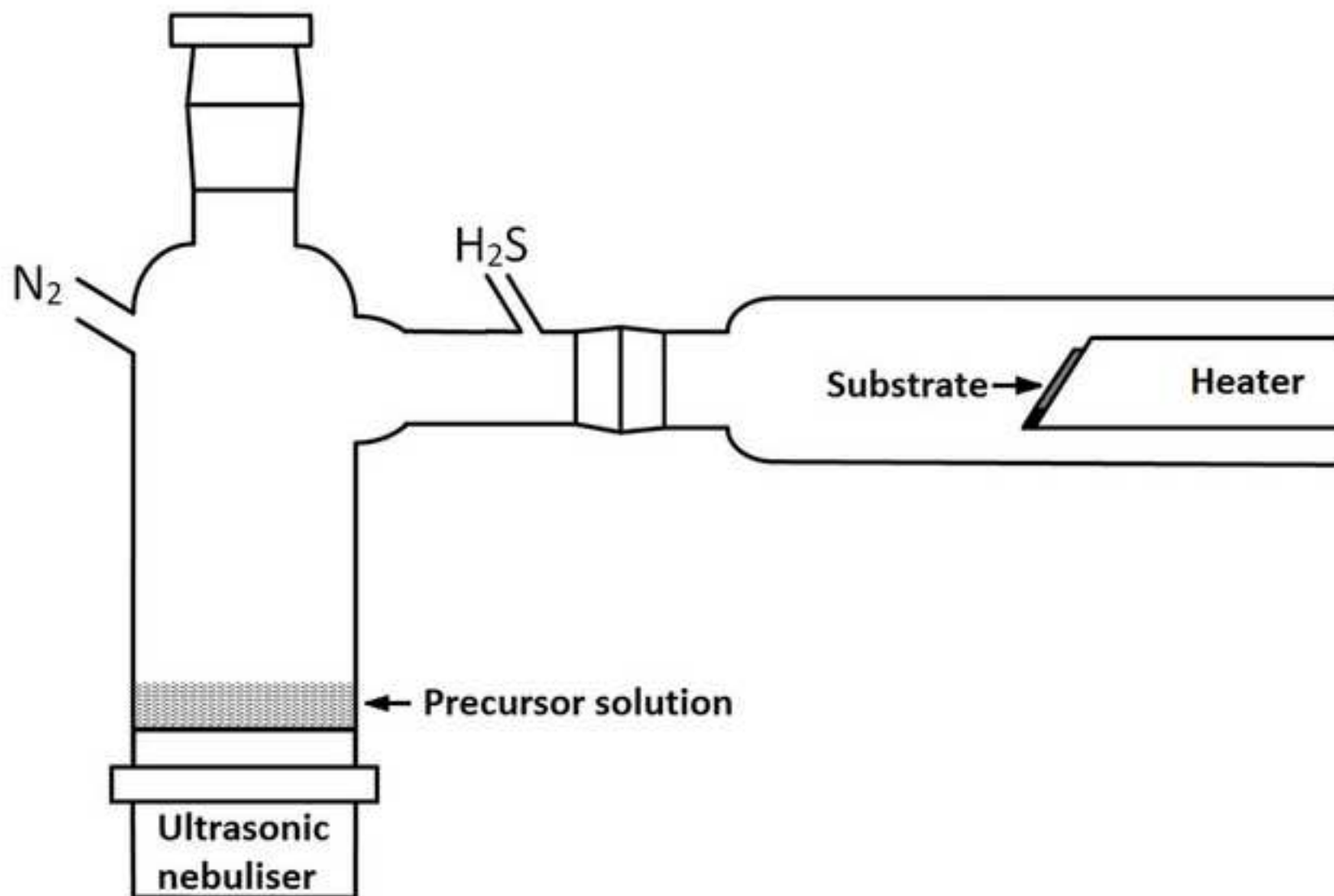
Figure1
Click here to download high resolution image

Figure3
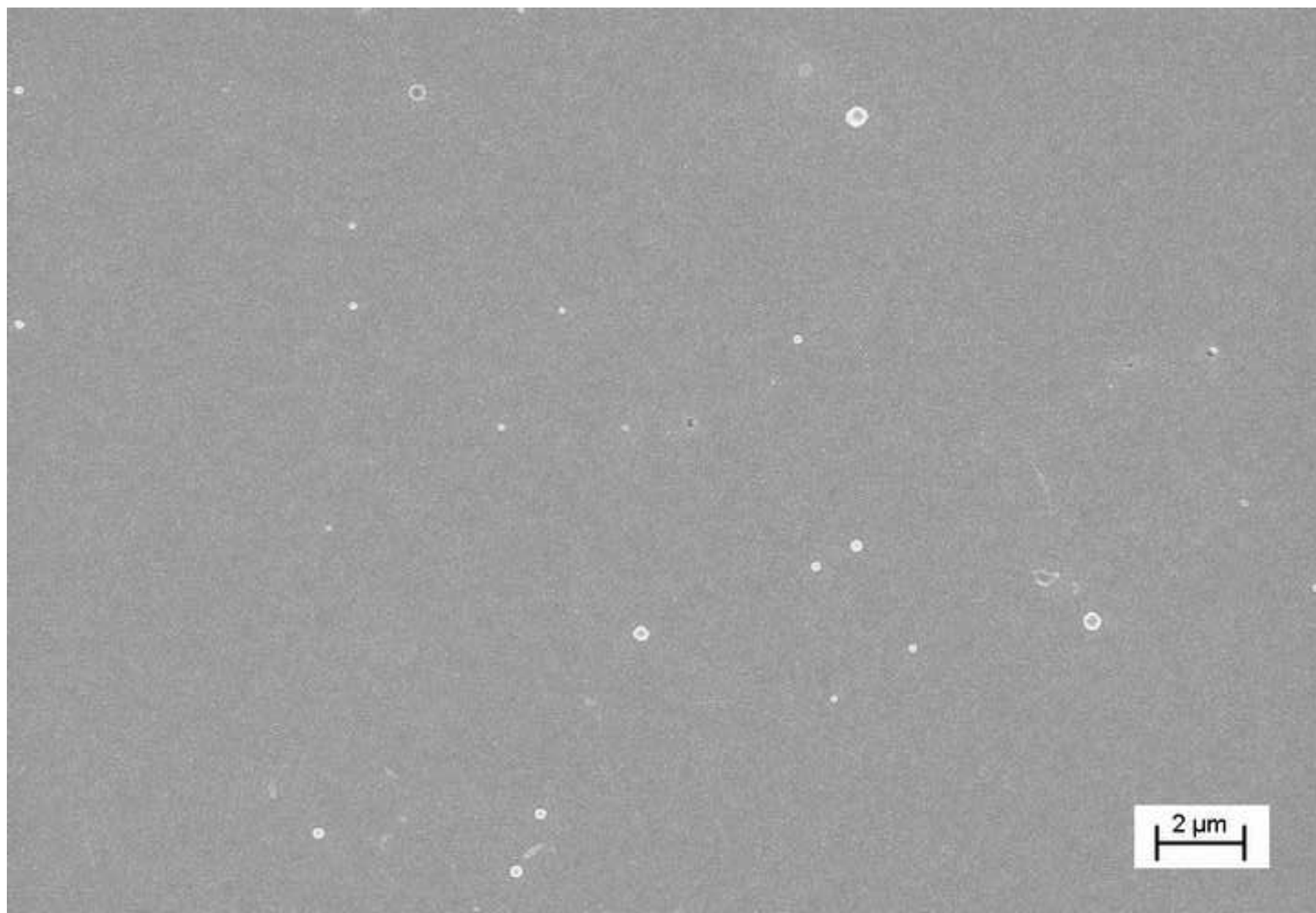**Click here to download high resolution image**

Figure5
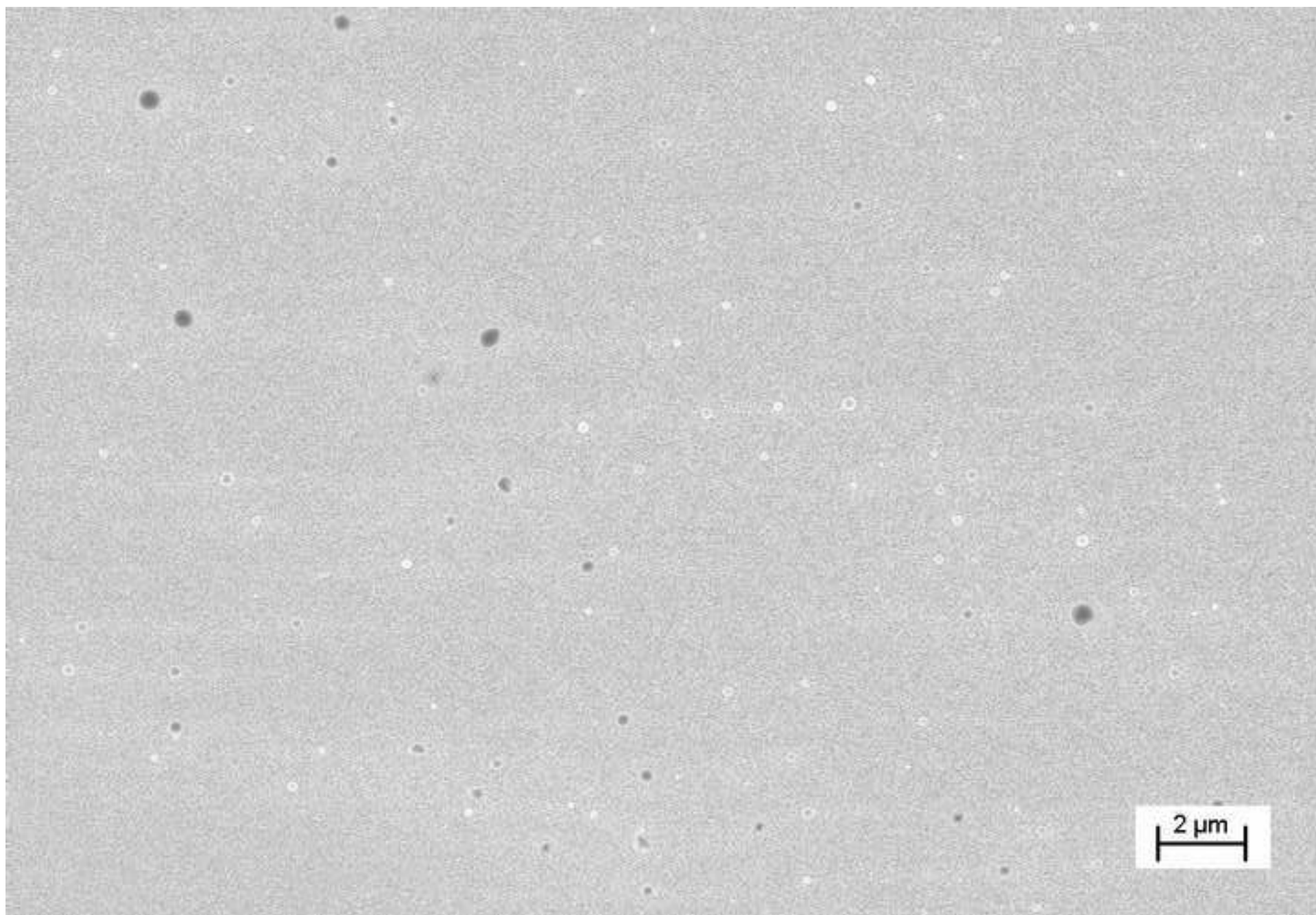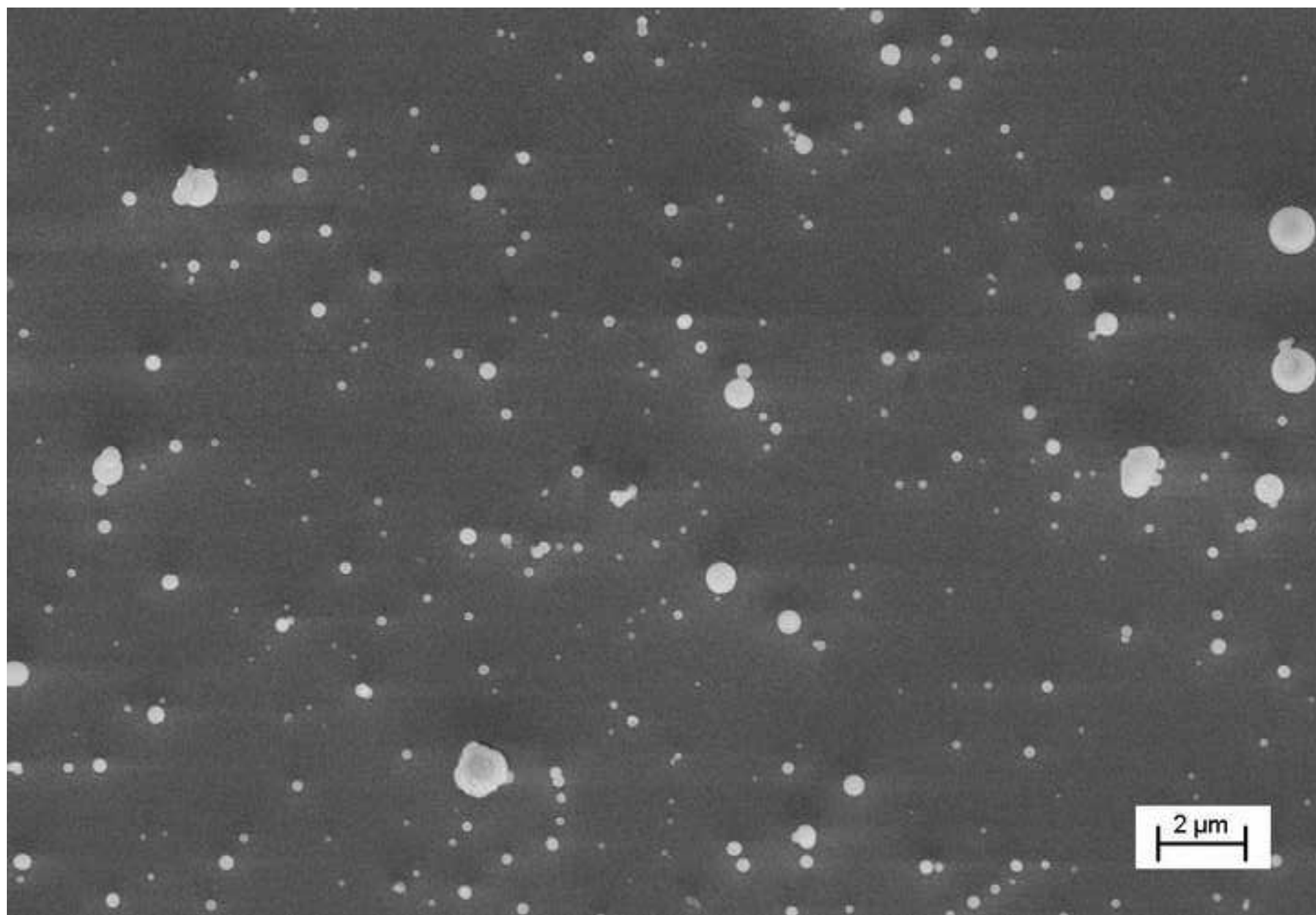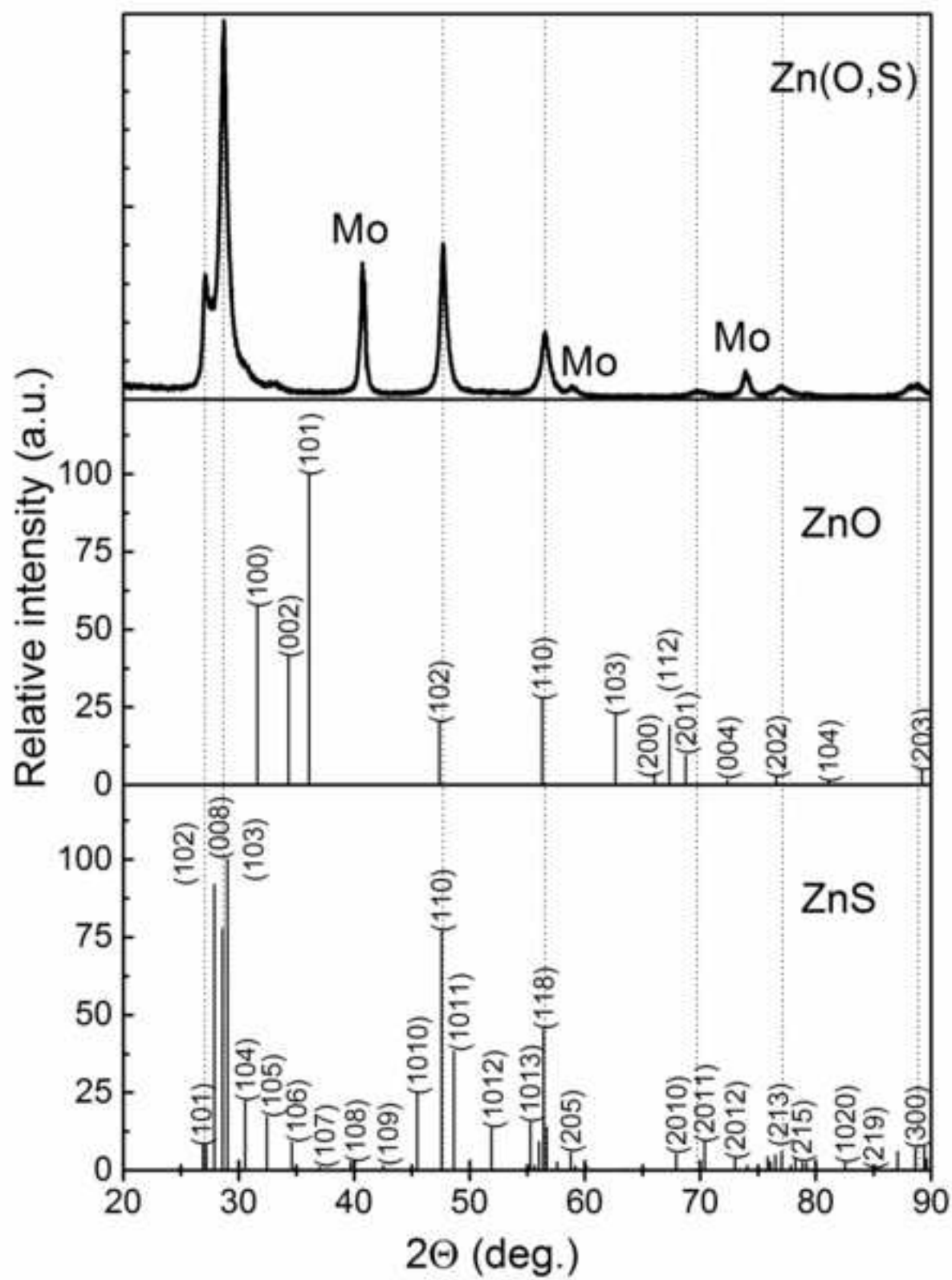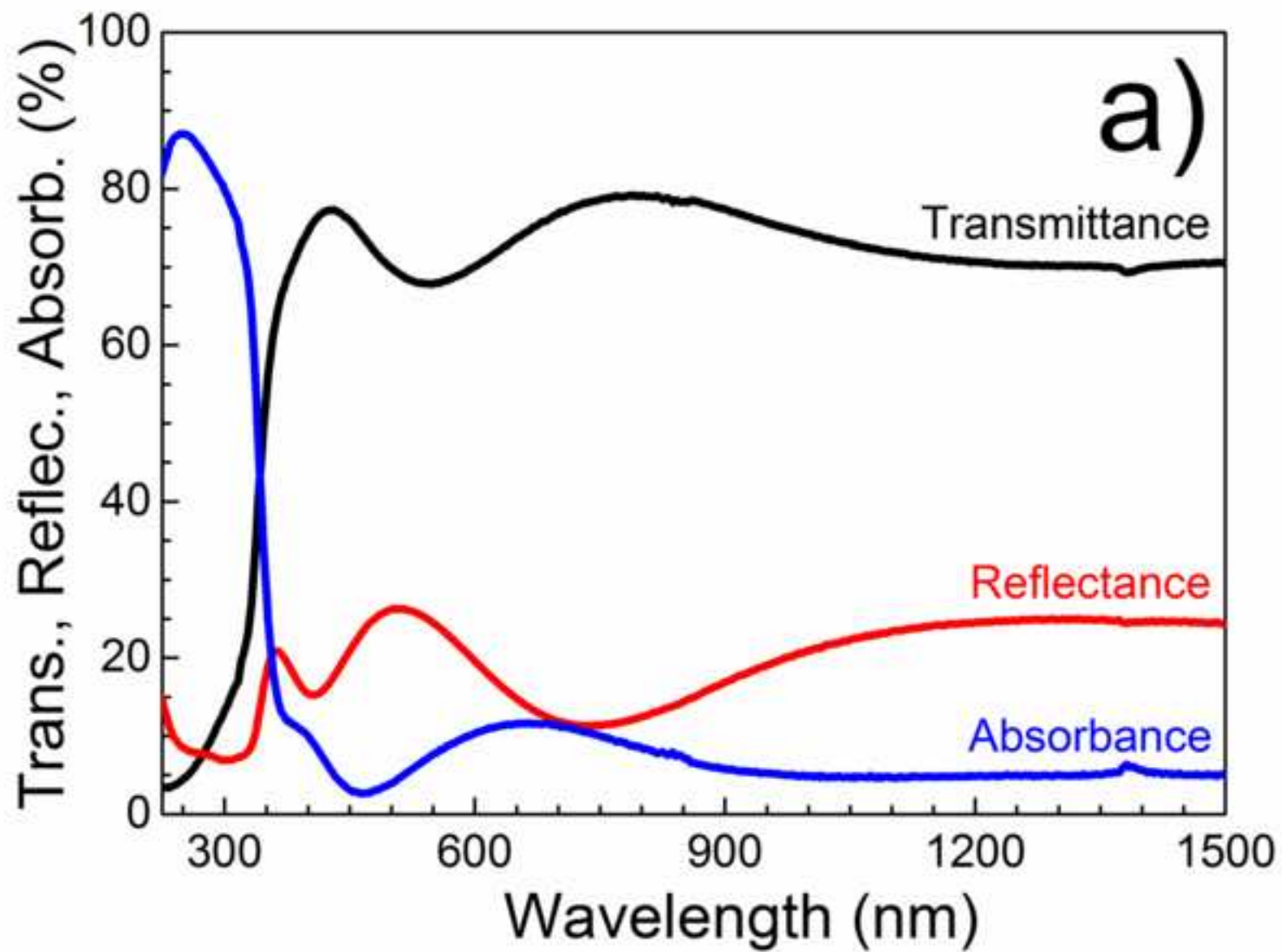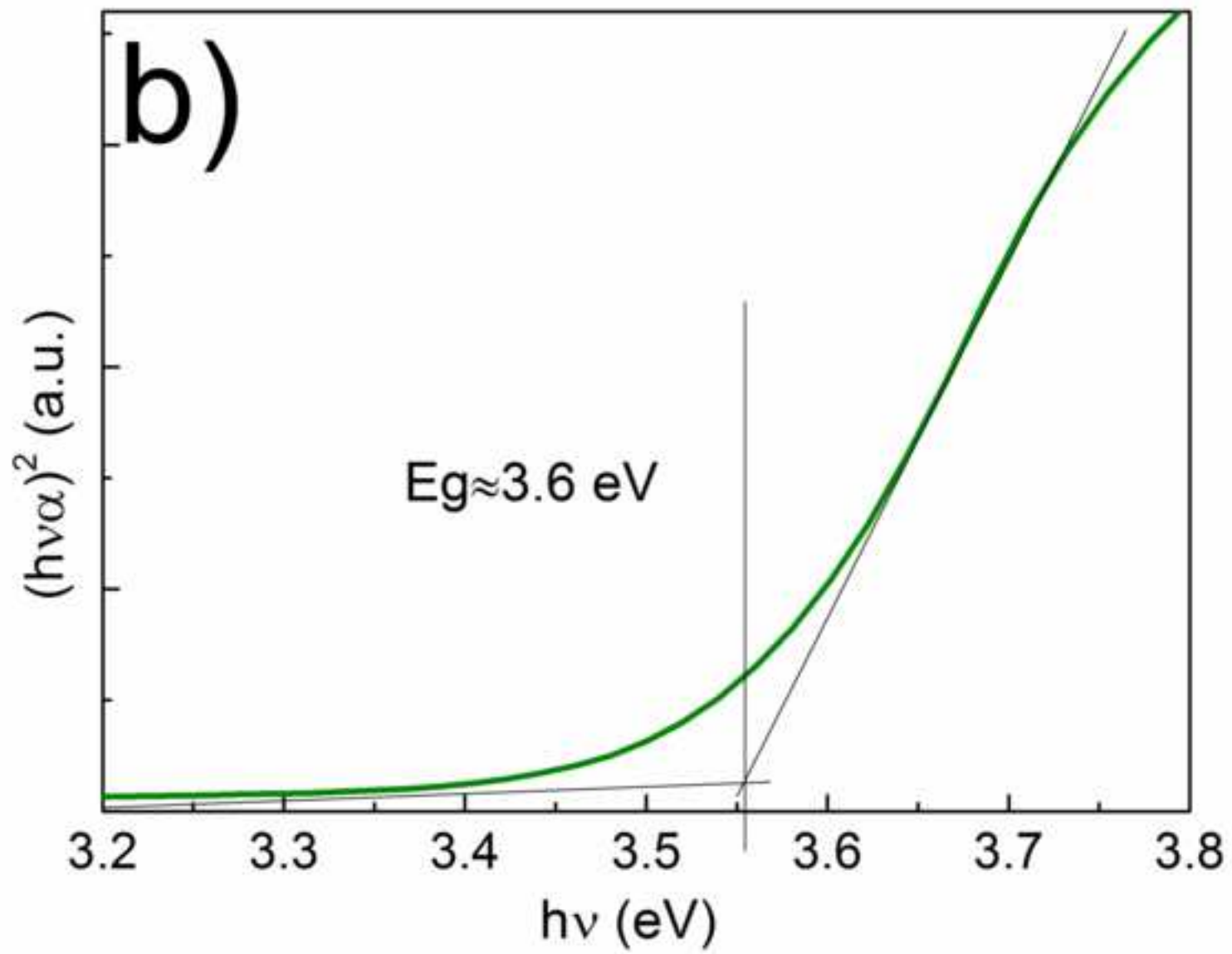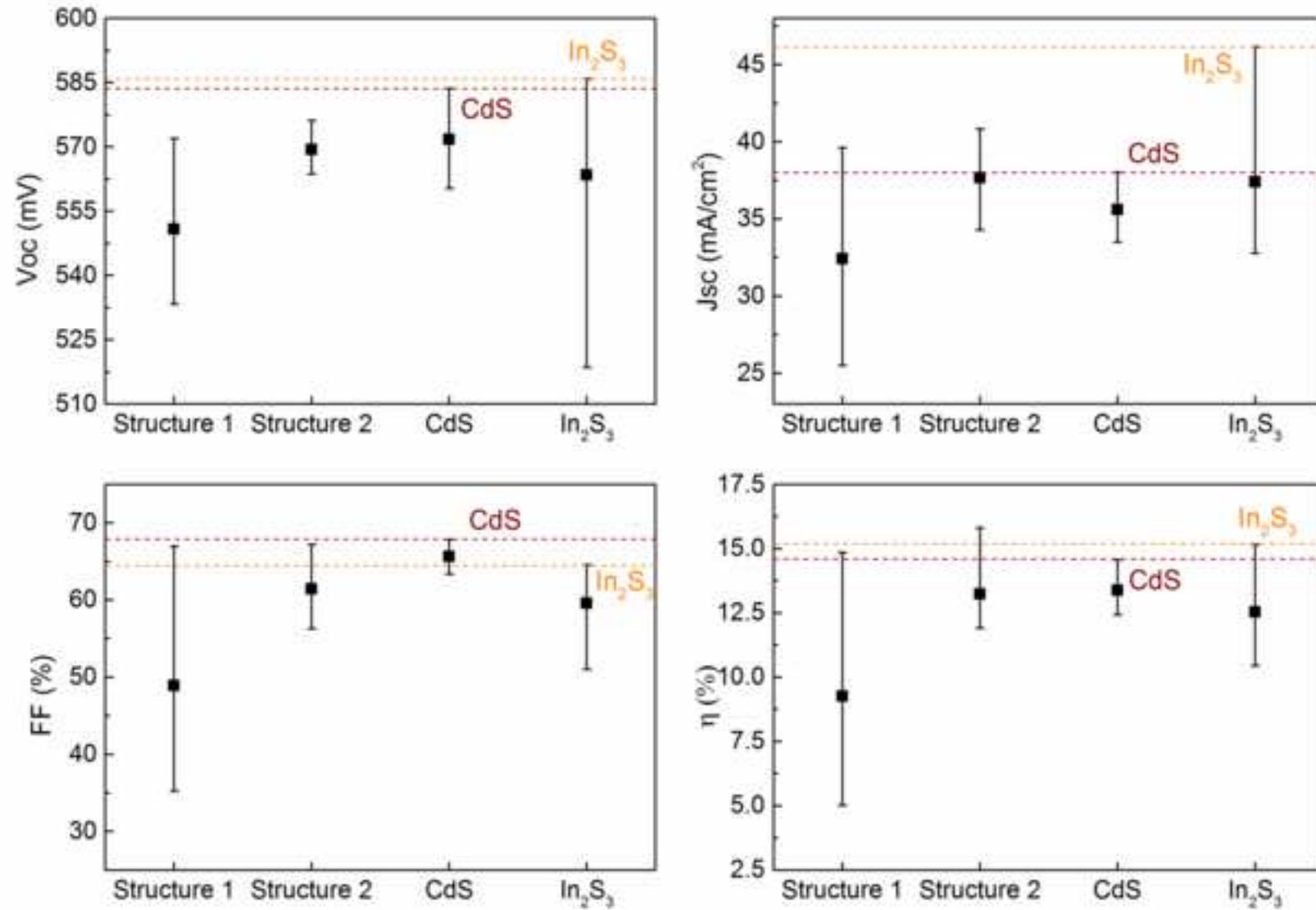**Click here to download high resolution image**

Figure6
Click here to download high resolution image